Chapter 4

Radiative transfer

Fundamentally, a spectrum is nothing more than a record of the number of photons counted in wavelength bins. Yet, with the application of a few simple physical principles, a basic information can be gleaned about the material emitting and absorbing the photons. To do so first requires an understanding of the basic quantities describing the propagation and observation of radiation. In addition, the a basic principles of radiative transfer, a description of how photons propagate through matter, is required.

In this chapter, we introduce a select few fundamental aspects of radiation fields, including specific intensity and flux. We also introduce the basic macroscopic principles of radiative transfer, especially focusing on absorption through matter. We then discuss the simple case of the one–dimensional transfer equation for pure absorption. Partial covering of the background source is also addressed.

Additional suggested resources that extend beyond the scope of this chapter are the books by Shu (1991), Peraiah (2002), and Rybicki & Lightman (2004), and by Novotny (1973), Gray (1992), Emerson (1996), and Mihalas (1978).

4.1 The radiation field

A full description of a radiation field requires both the energy (i.e., magnitude) and propagation direction of photons. Thus, the radiation field is a vector field. Let the propagation direction of a "beam" of photons be denoted by the unit vector $\hat{\mathbf{s}}$. In most applications, the $\hat{\mathbf{s}}$ direction of a beam of photons under consideration will be the line of sight to the observer.

The unit vector $\hat{\mathbf{s}}$ is most conveniently written in terms of the orthogonal unit base vectors of the Cartesian coordinate system

$$\hat{\mathbf{s}} = \cos\alpha\,\hat{\mathbf{i}} + \cos\beta\,\hat{\mathbf{j}} + \cos\gamma\,\hat{\mathbf{k}}, \tag{4.1}$$

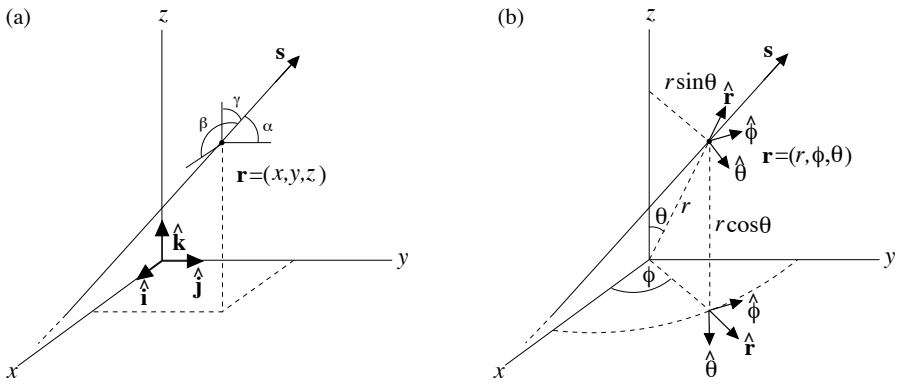

Figure 4.1: The unit vector $\hat{\mathbf{s}}$ represents a propagating "beam" of radiation that passes through point $\mathbf{r}$ in some arbitrary direction. (*a*) In the Cartesian coordinate system the point $\mathbf{r}$ is represented by the ordered pair (x, y, z). Unit vector $\hat{\mathbf{s}}$ is written in terms of the orthogonal unit base vectors $\hat{\mathbf{i}}$, $\hat{\mathbf{j}}$, and $\hat{\mathbf{k}}$. At the point $\mathbf{r}$, the direction cosine angles α, β, and γ are illustrated. (*b*) In the spherical coordinate system the point $\mathbf{r}$ is represented by the ordered pair (r, ϕ, θ), where r is the radial distance from the origin, ϕ is the azimuthal angle that sweeps counterclockwise from $0 \le \phi \le 2\pi$ rotated around the z axis ($\hat{\mathbf{k}}$ vector) with $\phi = 0$ in the $\hat{\mathbf{i}}$ direction, and θ is the polar (or zenith) angle that sweeps from the $\hat{\mathbf{k}}$ direction through the range $0 \le \theta \le \pi$ (to the $-\hat{\mathbf{k}}$ direction). The orthogonal unit base vectors are $\hat{\mathbf{r}}$, $\hat{\mathbf{\Phi}}$, and $\hat{\mathbf{\Theta}}$. Note that, unlike the Cartesian base vectors that are independent of $\mathbf{r}$, the direction of the spherical coordinate base vectors depend upon $\mathbf{r}$, as illustrated with the additional point in the $z = 0$ plane.

where $\cos\alpha$, $\cos\beta$, and $\cos\gamma$ are the direction cosines, which obey the relation $\cos^2\alpha + \cos^2\beta + \cos^2\gamma = 1$. By definition,

$$\hat{\mathbf{s}} \cdot \hat{\mathbf{i}} = \cos\alpha, \qquad \hat{\mathbf{s}} \cdot \hat{\mathbf{j}} = \cos\beta, \qquad \hat{\mathbf{s}} \cdot \hat{\mathbf{k}} = \cos\gamma. \tag{4.2}$$

The relationship between Cartesian and spherical coordinates is

$$\begin{aligned} x &= r\sin\theta\cos\phi & r &= (x^2 + y^2 + z^2)^{1/2} \\ y &= r\sin\theta\sin\phi & \theta &= \cos^{-1}(z/r) \\ z &= r\cos\theta & \phi &= \tan^{-1}(y/x), \end{aligned} \tag{4.3}$$

and the relationship between the unit base vectors between the two coordinate systems is

$$\begin{aligned} \hat{\mathbf{i}} &= \sin\theta\cos\phi\,\hat{\mathbf{r}} + \cos\theta\cos\phi\,\hat{\mathbf{\Theta}} - \sin\phi\,\hat{\mathbf{\Phi}} \\ \hat{\mathbf{j}} &= \sin\theta\sin\phi\,\hat{\mathbf{r}} + \cos\theta\sin\phi\,\hat{\mathbf{\Theta}} + \cos\phi\,\hat{\mathbf{\Phi}} \\ \hat{\mathbf{k}} &= \cos\theta\,\hat{\mathbf{r}} - \sin\theta\,\hat{\mathbf{\Theta}} \\ \hat{\mathbf{r}} &= \sin\theta\cos\phi\,\hat{\mathbf{i}} + \sin\theta\sin\phi\,\hat{\mathbf{j}} + \cos\theta\,\hat{\mathbf{k}} \\ \hat{\mathbf{\Theta}} &= \cos\theta\cos\phi\,\hat{\mathbf{i}} + \cos\theta\sin\phi\,\hat{\mathbf{j}} - \sin\theta\,\hat{\mathbf{k}} \\ \hat{\mathbf{\Phi}} &= -\sin\phi\,\hat{\mathbf{i}} + \cos\phi\,\hat{\mathbf{j}}. \end{aligned} \tag{4.4}$$

As illustrated in Figure 4.1, the unit base vector directions in the Cartesian system are defined parallel to the principle axes of the system. As such, they are independent of the location $\mathbf{r} = (x, y, z) = (r, \theta, \phi)$. On the contrary, in the spherical coordinates system the directions of the unit base vectors depend upon the position $\mathbf{r}$. The (θ, ϕ) dependence of $\hat{\mathbf{r}}$, $\hat{\mathbf{\Theta}}$, and $\hat{\mathbf{\Phi}}$ are given in Eq. 4.4.

Detailed descriptions of the radiation field incorporate not only the energy and direction, but also angular averages, or moments. These moments relate to how a beam traveling in the $\hat{\mathbf{s}}$ direction propagates into a two–dimensional angular element called the solid angle. The general definition of solid angle, Ω, is the ratio of the physical area through which the beam passes to the distance squared, D^2, from either the source or the observer's location, i.e., $\Omega = A/D^2$, depending upon the application of the analysis. In the spherical coordinate system, the area element on a sphere of radius R is

$$\mathbf{dA} = dA\,\hat{\mathbf{n}} = R^2 \sin\theta\, d\theta\, d\phi\, \hat{\mathbf{n}}, \tag{4.5}$$

where $\hat{\mathbf{n}} = \hat{\mathbf{r}}$ is the vector normal to the sphere surface at location R, ϕ, θ.

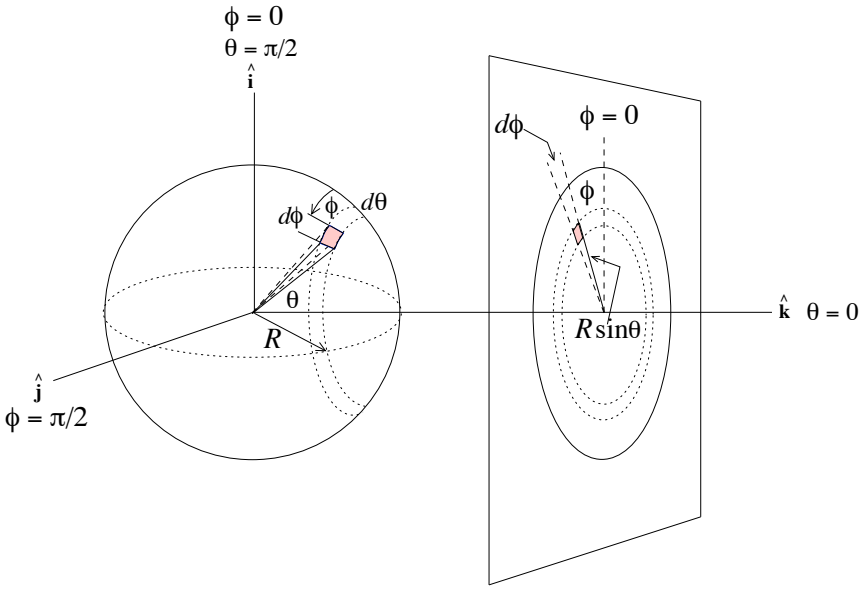

Figure 4.2: A schematic of the area element, dA, on a sphere or radius R. The area element can be placed in the context of an annulus of angular width $d\theta$ about the azimuth angle ϕ (rotation about the $\hat{\mathbf{k}}$ vector). The arc length on the sphere over angle $d\theta$ (the zenith angle) is $R\,d\theta$, since the arc lies on a great circle of the sphere. The arc length in the azimuthal direction is $R\sin\theta\, d\phi$. This latter arc length does not lie on a great circle, but on a circle of radius $R\sin\theta$, as illustrated on the two–dimensional collapsed view from the $\hat{\mathbf{k}}$ point of view. The area element is the product of the two arc lengths and has unit vector direction $\hat{\mathbf{n}}$ normal to the surface, i.e., $\hat{\mathbf{r}}$.

The area element is illustrated in Figure 4.2. The (ϕ, θ) integration limits required to obtain the surface area of the sphere are $0 \leq \theta \leq \pi$ (the polar

angle, counter clockwise from the $\hat{\mathbf{k}}$ ($\theta = 0$) to the $-\hat{\mathbf{k}}$ ($\theta = -\pi$) direction) and $0 \leq \phi \leq 2\pi$ (the azimuthal angle, rotation about the pole, or $\hat{\mathbf{k}}$ direction, with $\phi = 0$ in the $\hat{\mathbf{i}}$ direction). Viewed from the center of the sphere, the solid angle subtended by the surface area element is

$$d\Omega = \frac{dA}{R^2} = \sin\theta \, d\theta \, d\phi. \tag{4.6}$$

The same area element, as viewed by an observer located at distance D along a line of sight vector direction $\hat{\mathbf{s}}$ passing through the area element on the sphere, will subtend solid angle

$$d\Omega = \frac{dA}{D^2} = \frac{R^2(\hat{\mathbf{s}} \cdot \hat{\mathbf{n}}) \sin\theta \, d\theta \, d\phi}{D^2}, \tag{4.7}$$

where dA is the projected area from the observer's perspective. If the angle between $\hat{\mathbf{s}}$ and the area normal $\hat{\mathbf{n}}$ is ψ, then $\hat{\mathbf{s}} \cdot \hat{\mathbf{n}} = \cos\psi$.

4.1.1 Specific intensity

Consider a point in space at $\mathbf{r} = (r, \phi, \theta)$ at time t. Let electromagnetic radiation propagating in $\hat{\mathbf{s}}$ direction pass through this point. The fundamental quantity describing the propagation of radiation is the specific intensity, $\mathcal{I}_\lambda$. The specific intensity is defined as the incremental amount of energy, $d\epsilon_\lambda$, transported in direction $\hat{\mathbf{s}}$ by radiation of wavelength range $\lambda \rightarrow \lambda + d\lambda$ passing through an infinitesimal projected area centered on $\mathbf{r}$ into solid angle $d\Omega$ in time interval dt,

$$d\epsilon_\lambda = \mathcal{I}_\lambda \, (\hat{\mathbf{s}} \cdot \hat{\mathbf{n}}) \, dA \, d\Omega \, d\lambda \, dt, \tag{4.8}$$

where $\hat{\mathbf{n}}$ is the normal direction of the area element, dA. The units of specific intensity are [erg cm^{-2} sec^{-1} rad^{-2} Å^{-1}].

This complex definition is required because a "beam" of radiation is not coherent (in both the wavelength phases and in the precise directions of the individual photons– they are not plane parallel). Thus, even if the propagation direction can be well defined, the precise measure of the energy transported at any location along the beam requires accounting of the non–parallel photon paths, which results in some photons exiting the beam and other photons entering the beam at various line of sight locations.

A schematic is presented in Figure 4.3*a* for which $(\hat{\mathbf{s}} \cdot \hat{\mathbf{n}}) \, dA = dA$, i.e., $\hat{\mathbf{s}}$ is parallel to $\hat{\mathbf{n}}$ and $\hat{\mathbf{s}} \cdot \hat{\mathbf{n}} = 1$. This scenario provides a one dimensional description of the phenomena of radiative energy transport. Figure 4.3*b* provides a schematic in which the direction of propagation, $\hat{\mathbf{s}}$, subtends and angle θ with the area element normal. In this case $(\hat{\mathbf{s}} \cdot \hat{\mathbf{n}}) \, dA = dA \cos\theta$.

4.1.2 The flux integral

In an astronomical experiment, flux is the energy captured per unit time per unit area. Flux is a vector. If a source emits light isotropically, for example,

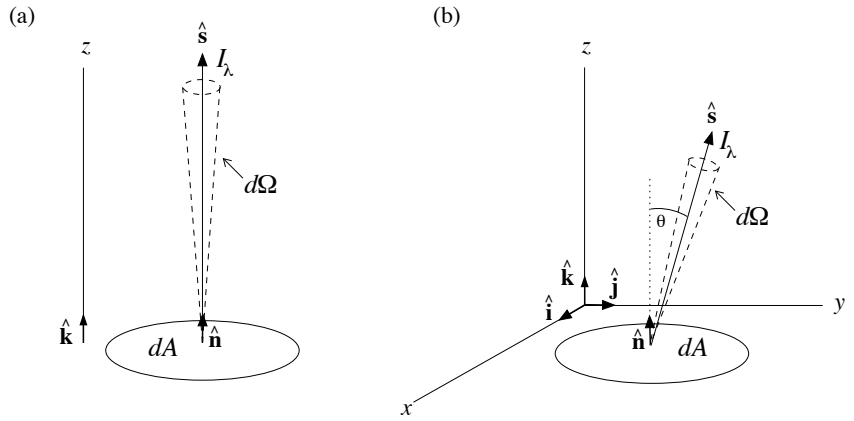

Figure 4.3: (*a*) A schematic of a pencil beam of radiative energy of specific intensity $\mathcal{I}_\lambda$ propagating in the $\hat{\mathbf{s}}$ direction through area element dA into solid angle $d\Omega$. In this example, the propagation is parallel to $\hat{\mathbf{n}}$, the area normal unit vector, and parallel to a (or the) principle axis of the coordinate system (z axis in the $\hat{\mathbf{k}}$ direction). This illustrates the case in which the geometry is defined with respect to the propagation direction. (*b*) In a geometry in which the orientation of the area element is defined, the propagation direction may not be parallel to $\hat{\mathbf{n}}$. In such cases, the radiative energy $d\epsilon_\lambda$ transported by the beam of specific intensity $\mathcal{I}_\lambda$ in the $\hat{\mathbf{s}}$ direction is modulated by the factor $\hat{\mathbf{s}} \cdot \hat{\mathbf{n}} = \cos\theta$, which accounts for the projection of the area element, dA, along the line of sight.

the measured flux comprises only those photons emitted in the direction of the observer, i.e., in the $\hat{\mathbf{s}}$ direction. The flux integral is

$$\mathbf{F}_\lambda = \iint_\Omega \mathcal{I}_\lambda \, \hat{\mathbf{s}} \, d\Omega, \tag{4.9}$$

with units [erg cm^{-2} sec^{-1} Å^{-1}]. Flux is the first moment of the specific intensity. The solid angle is determined from the perspective of the observer. However, the integral is often most easily evaluated if the integration is taken over the source object itself (see below). For specific intensity propagating in the line of sight direction $\hat{\mathbf{s}}$ through an area element $\mathbf{dA} = dA\,\hat{\mathbf{n}}$ having observed solid angle $d\Omega$, the magnitude of the line of sight component of the flux is

$$F_\lambda = \iint_\Omega \mathcal{I}_\lambda \, (\hat{\mathbf{s}} \cdot \hat{\mathbf{n}}) \, d\Omega. \tag{4.10}$$

In Cartesian coordinates, the line of sight vector can be expressed $\hat{\mathbf{s}} = \cos\alpha\,\hat{\mathbf{i}} + \cos\beta\,\hat{\mathbf{j}} + \cos\gamma\,\hat{\mathbf{k}}$, where $\cos\alpha$, $\cos\beta$, and $\cos\gamma$ are the direction cosines. We also can write the flux as the vector sum

$$\mathbf{F}_\lambda = F_\lambda^x\,\hat{\mathbf{i}} + F_\lambda^y\,\hat{\mathbf{j}} + F_\lambda^z\,\hat{\mathbf{k}}, \tag{4.11}$$

where F_λ^x, F_λ^y, and F_λ^z respectively provide the $\hat{\mathbf{i}}$, $\hat{\mathbf{j}}$, and $\hat{\mathbf{k}}$ components of the net rate of radiative energy per unit wavelength per unit time crossing a projected

unit area for a beam propagating in the $\hat{\mathbf{s}}$ direction. The flux vector components are then

$$\begin{aligned} F_\lambda^x &= \iint_\Omega \mathcal{I}_\lambda \left(\hat{\mathbf{i}} \cdot \hat{\mathbf{n}}\right) d\Omega \\ F_\lambda^y &= \iint_\Omega \mathcal{I}_\lambda \left(\hat{\mathbf{j}} \cdot \hat{\mathbf{n}}\right) d\Omega \\ F_\lambda^z &= \iint_\Omega \mathcal{I}_\lambda \left(\hat{\mathbf{k}} \cdot \hat{\mathbf{n}}\right) d\Omega, \end{aligned} \tag{4.12}$$

where the first unit vector in the dot product is the $\hat{\mathbf{i}}$, $\hat{\mathbf{j}}$, or $\hat{\mathbf{k}}$ projection of the $\hat{\mathbf{s}}$ vector in Eq. 4.9, and the second unit vector, $\hat{\mathbf{n}}$, is the unit area vector through which the beam passes. If the beam is passing through the surface of a sphere centered at the origin of the coordinate system, then the unit area vector is $\hat{\mathbf{n}} = \hat{\mathbf{r}}$, and we have

$$\begin{aligned} \hat{\mathbf{i}} \cdot \hat{\mathbf{n}} &= \hat{\mathbf{i}} \cdot \hat{\mathbf{r}} = \cos\alpha = \sin\theta\cos\phi \\ \hat{\mathbf{j}} \cdot \hat{\mathbf{n}} &= \hat{\mathbf{j}} \cdot \hat{\mathbf{r}} = \cos\beta = \sin\theta\sin\phi \\ \hat{\mathbf{k}} \cdot \hat{\mathbf{n}} &= \hat{\mathbf{k}} \cdot \hat{\mathbf{r}} = \cos\gamma = \cos\theta, \end{aligned} \tag{4.13}$$

where θ and ϕ are the standard spherical coordinates.

For example, consider the flux of radiation propagating in the outward radial direction from a central point $\mathbf{r}$ so that $\hat{\mathbf{s}} = \hat{\mathbf{n}}$ everywhere on the surface of a unit sphere. The radial component of the flux captured over all solid angle is then

$$F_\lambda^r = \oint \mathcal{I}_\lambda \left(\hat{\mathbf{n}} \cdot \hat{\mathbf{n}}\right) d\Omega. = \oint \mathcal{I}_\lambda \, d\Omega = 4\pi J_\lambda. \tag{4.14}$$

Thus, we see that the radial flux normalized by the integral over all solid angle, $F_\lambda^r/4\pi$, is equivalent to the mean intensity,

$$J_\lambda = \frac{\oint \mathcal{I}_\lambda \, d\Omega}{\oint d\Omega} = \frac{1}{4\pi} \oint \mathcal{I}_\lambda \, d\Omega, \tag{4.15}$$

about the central point $\mathbf{r}$. The mean intensity is a useful quantity that provides the mean of specific intensity enclosed in an arbitrary volume.

4.1.3 The astrophysical flux

The astrophysical flux, $\mathcal{F}_\lambda$, quantifies the component of the total surface flux emitted by a source that will be intercepted by an observer. A randomly placed observer at distance $D \gg R_s$ from the source, where R_s is the source radius, will intercept photons that originate from only the near–side hemisphere of the source and are emitted in the direction toward the observer.

Assume the observer is located along the $+z$ axis, such that the line of sight from the source is $\hat{\mathbf{s}} = \hat{\mathbf{k}}$ (we assume all beams reaching the observer are parallel). The general geometry of this scenario is illustrated in Figure 4.2 with the observer placed at $\theta = 0$. Also assume the emitted specific intensity is isotropic and time independent, i.e., $\mathcal{I}_\lambda = \mathcal{I}_\lambda(R_s)$. From Eqs. 4.12, 4.13, and 4.6,

$$\mathcal{F}_\lambda = \iint_\Omega \mathcal{I}_\lambda(R_s)(\hat{\mathbf{k}} \cdot \hat{\mathbf{n}})\, d\Omega = \int_0^{2\pi}\int_0^{\pi/2} \mathcal{I}_\lambda(R_s)\cos\theta\sin\theta\, d\theta\, d\phi, \tag{4.16}$$

where $d\Omega = dA_s/R_s^2 = \sin\theta\, d\theta\, d\phi$ on the source surface, and where the integration over the polar angle ($0 \le \theta \le \pi/2$) includes only the observable hemisphere. Evaluating, we find

$$\mathcal{F}_\lambda = 2\pi\mathcal{I}_\lambda(R_s)\left\{\frac{1}{2}\sin^2\theta\,\Big|_0^{\pi/2}\right\} = \pi\mathcal{I}_\lambda(R_s). \tag{4.17}$$

Thus, assuming the specific intensity at the surface is isotropic, the observable component of the total surface flux emitted by a spherical source is equal to the geometric factor π times the specific intensity at the surface.

4.1.4 The observed flux

The observed flux is a measurement of the energy per unit area per unit wavelength per unit time intercepted by a detector. As such the observed flux necessarily depends upon the solid angle of the collected beam.

All instruments have a limiting resolution, a minimum solid angle, Ω_r, over which they can collect focused light. For ground–based instruments, the resolution is usually limited by the atmospheric seeing (FWHM angular width of $\sim 1''$). If an object subtends a solid angle, Ω_s, less than that of the instrumental resolution, the object is said to be unresolved; however, if $\Omega_s > \Omega_r$, the object is said to be resolved. As we demonstrate below, the observed flux of a resolved object is independent of its distance from the observer, whereas the observed flux of an unresolved object depends upon both its distance and its radius, R_s.

Resolved sources

We first consider a resolved source. Assume an instrument has focal length f and limiting angular resolution that projects to an area element on the detector $A_r = \pi r_r^2$, where r_r is the half width half maximum of the angular resolution element. As illustrated in Figure 4.4*a*, the minimum solid angle over which light can be collected is $\Omega_r = A_r/f^2 = \pi r_r^2/f^2$. Consider a spherical emitting source of radius R_s at a distance D from the focal point of the instrument that subtends a total solid angle $\Omega_s > \Omega_r$. The source is resolved. The collected light in each resolution element is limited to an area on the source $A_s = \Omega_r D^2$ (the equality presumes $D \gg R_s$).

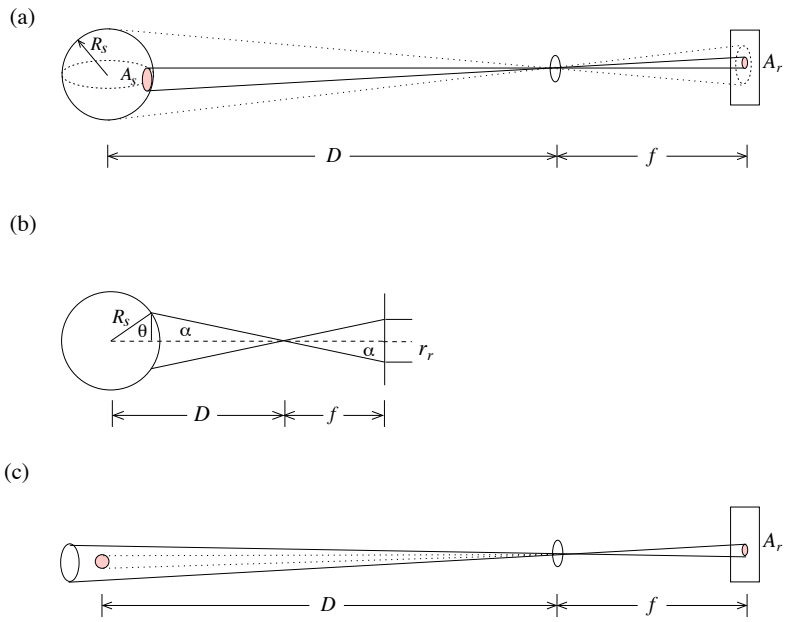

Figure 4.4: (*a*) The relationships between the area of the resolution element, A_r, of an instrument with focal length f and the observed area on the source, A_s, of radius R_s at distance D when the source is resolved. The minimum solid angle over which light can be collected is $\Omega_r = A_r/f^2 = \pi r_r^2/f^2$, which projects to area $A_s = \Omega_r D^2$ on the source. (*b*) An expanded view of the geometry for the resolved source showing the relationship between the angle θ, distance, focal length, source radius, and linear size of the instrument resolution element. (*c*) Similar to the schematic in panel (*a*), but for an unresolved source, i.e., $\Omega_s < \Omega_r$. For all panels, Ω_r is illustrated with the solid cone and Ω_s is illustrated with the dot–dot cone.

To compute the observed flux from the resolved source, we invoke the identical geometric relationships between source and observer applied in § 4.1.3 to compute the astrophysical flux, $\mathcal{F}_\lambda$. The flux integral is similar to that of Eq. 4.16, except that (1) the solid angle is determined from the position of the observer, and (2) the integration over the solid angle is limited to the area A_s on the source.

As illustrated in Figure 4.2, $dA_s = R_s^2 \sin\theta\, d\theta\, d\phi$ is the area element on the source. From a distance D along $+z$ axis the observed solid angle element is

$$(\hat{\mathbf{k}} \cdot \hat{\mathbf{n}})\, d\Omega = \cos\theta\, \frac{dA_s}{D^2} = \frac{R_s^2}{D^2} \cos\theta \sin\theta\, d\theta\, d\phi. \tag{4.18}$$

The integration limits are determined from the geometric relationships illustrated in Figure 4.4*b*. From similar triangles reflected about the focal point, $\tan\alpha = (r_r/f) = R_s \sin\theta/(D - R_s\cos\theta)$. Provided $D \gg R_s$, we obtain the polar angle limit of integration corresponding to the solid angle of a resolution

element,

$$\theta_r = \sin^{-1}\left(\frac{D}{R_s}\tan\alpha\right) = \sin^{-1}\left(\frac{D}{R_s}\frac{r_r}{f}\right). \tag{4.19}$$

The observed flux collected at a distance D is then

$$F_\lambda = \iint_\Omega \mathcal{I}_\lambda(R_s)(\hat{\mathbf{k}}\cdot\hat{\mathbf{n}})\,d\Omega = \frac{R_s^2}{D^2}\int_0^{2\pi}\int_0^{\theta_r}\mathcal{I}_\lambda(R_s)\cos\theta\sin\theta\,d\theta\,d\phi. \tag{4.20}$$

Carrying out the integration, we obtain

$$\begin{aligned} F_\lambda &= \pi\mathcal{I}_\lambda(R_s)\frac{R_s^2}{D^2}\sin^2\left\{\sin^{-1}\left(\frac{D}{R_s}\frac{r_r}{f}\right)\right\} \\ &= \pi\mathcal{I}_\lambda(R_s)\frac{r_r^2}{f^2} = \Omega_r\mathcal{I}_\lambda(R_s) = \frac{r_r^2}{f^2}\mathcal{F}_\lambda = \Omega_r\frac{\mathcal{F}_\lambda}{\pi}. \end{aligned} \tag{4.21}$$

When an object is resolved, the observed flux provides a direct measurement of the source specific intensity and the astrophysical flux modulo the solid angle of the resolution element, but independent to both the radius of and distance to the source.

Unresolved source

Now, we consider an unresolved object with $\Omega_s < \Omega_r$, as illustrated in Figure 4.4*c*. The emerging intensity from the full hemisphere of the source will be recorded in a single resolution element. The calculation is identical to Eq. 4.20, except we replace θ_r with $\pi/2$ for the upper limit of integration. Evaluating the flux integral, we obtain

$$F_\lambda = \pi\mathcal{I}_\lambda(R_s)\frac{R_s^2}{D^2} = \Omega_s\mathcal{I}_\lambda(R_s) = \frac{R_s^2}{D^2}\mathcal{F}_\lambda = \Omega_s\frac{\mathcal{F}_\lambda}{\pi}. \tag{4.22}$$

The observed flux of an unresolved source yeilds a measurement of the source specific intensity and astrophysical flux modulo the solid angle of the source; thus one must know both the source size and distance.

In summary, we see that, whether the source is resolved or unresolved, the observed flux is $\Omega(\mathcal{F}_\lambda/\pi)$, where $\mathcal{F}_\lambda$ is the astrophysical flux and Ω is the solid angle of the collected beam. In the case of a resolved source, the solid angle is the solid angle of the detector resolution element so that the observed flux is independent of both the source size and distance. In the case of an unresolved source, the solid angle is that subtended by the disk of the source.

Applied Assumptions

Note that several assumptions have been applied in the above examples, i.e., an isotropic, time independent, and spherical emitting source with $D \gg R_s$. In practice, these assumptions are so commonly applied that they are implicit in most work presented in the astronomical literature.

In reality, the source may not emit isotropically, such that $\mathcal{I}_\lambda = \mathcal{I}_\lambda(R_s, \phi, \theta)$. If the source is not spherical, then $R_s = R(\phi, \theta)$. It is also possible that the emission (intensity and wavelength dependence) and/or the object's physical size and shape are time variable. Clearly, proper treatment of the flux integral can be far more complex than treated here.

4.2 Microscopic Absorption

Absorption can be described as a processes in which a given photon, and its energy, is removed from the radiation field by matter. The photon energy can be converted into either an increase in the internal energy of the absorbing atom, or into the kinetic energy of a free electron. Scattering is the process in which the direction of a photon is deflected, but the wavelength and energy are virtually unchanged. Both processes result in the photon in question being removed from its direction of propagation prior to the interaction. In this chapter, and throughout this book, we will focus on absorption processes. The three main aborption processes can be summarized as follows:

- *bound–bound transitions*: is the process in which an electron bound to an atom in a given orbit, absorbs the energy of an incident photon and in the process is raised to a higher energy orbit. The photon energy is removed from the radiation field and will temporarily remain internal to the atom (the atom is said to be in an excited state). The electron could initially have been in the ground state (lowest energy orbit) or already in an excited state. For bound–bound transitions to occur, the photon energy must equal (within in a narrow distribution) the energy difference between the allowed intitial and final bound states of the electron.

- *bound–free transitions*: also known as ionization, this is the processes in which a photon incident on an atom in a gas is absorbed by a bound electron, which is then ejected from the atom and becomes a free entity in the gaseous medium. As with bound–bound absorption, the electron initially could have been in the ground state or already in an excited state. The photon energy is converted into kinetic energy (deposited into the electron pool of the gas) less the energy required to electrically unbind the electron. For a bound–free transition to occur, the photon energy must be equal to or greater than the binding energy of the initial bound state of the electron.

- *free–free transitions*: is a process usually occurs in relatively higher density gas since it is a three body interaction. A free (unbound) electron in proximity to a neutral or ionized atom may absorb an incident photon. In this process, the electron kinetic energy is increased (whereas the total interaction energy and momentum are conserved by the three body process). As with bound–free absorption, free–free absorption couples the energy in the radiation field with the kinetic energy in the gas.

In Figure 12.4, schematics of bound–bound absorption (panel a), bound–free absorption (panel b), and free–free absorption are presented. In a very short time span (10^{-8} [sec]) following a bound–bound absorption, the atom will deexcited, emitting a photon in the process of the electron dropping to a lower energy state (orbit). This may result in multiple photons being emitted in multiple directions as the electron cascades through lower orbits on its way to the ground state, or it may result in the emission in a random direction of a photon of the same wavelength as the absorbed photon if the electron directly returns to its initial state. The probability that the emitted photons will be emitted in the propagation direction of the original absorbed photon is tiny. Thus, the observer measures a reduction in the flux of the photon source. Following bound–free absorption, the free electron is very quickly thermalized by the electron pool in the gas. Again, the observer measures a reduction in the flux of the photon source.

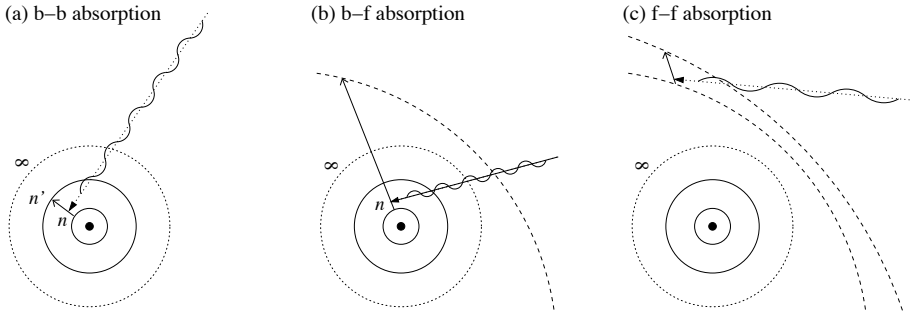

Figure 4.5: Schematic of the three primary atomic absorption transitions (a) Bound–bound (b–b) absorption from bound discrete state n to a higher energy bound discrete state, n'. (b) Bound–free (b–f) absorption, also known as ionization from discrete bound state n to a "continuous" free state. The free state can be treated as a hyperbolic orbit around the host atom. (c) Free–free (f–f) absorption, which is a three body process. A free electron in the proximity to an atom absorbs a photon and is raised to a higher energy state. Both free state can be treated as a hyperbolic orbits around the host atom.

Free–free transitions are a three–body process and are therefore sensitive to the gas density (occuring with greater frequency in higher density gas). The likelihood of free–free aborption increases rapidly at longer wavelength (lower photon energies. As such the optical depth to free–free absorption for visible and ultraviolet photons is virtually negligible except for in the most very dense environments. Since most all spectroscopic observations of cosmological objects involve the study of absorption at ultraviolet and optical wavelengths in the frame of the absorbing medium, we will focus our discussion on bound–bound and bound–free absorption.

4.3 Macroscopic Treatment

In the above sections we provided definitions for the specific intensity and flux, two macroscopic quantities of the radiation field. In the presence of matter (neutral, partially ionized, or fully ionized gas) the radiation field is modified via the processes of absorption, scattering, and/or emission. In most applications, the modifications result in emission or absorption features in an otherwise smoothly varying spectral energy distribution. It is the measurement of these features that provides insight into the physical conditions (ionization, chemical abundance, temperature, kinematics, etc) of the modifying matter.

Radiative transfer is a formalism of macroscopic physics that is founded upon the countless microscopic physical interactions between radiation and matter. The macroscopic variables that describe these processes are the extinction coefficient, the optical depth, the emission coefficient, and the source function. In general, these macroscopic variables are the sums of numerous microscopic conditions. However, in practice (as will be shown), the analysis of an individual absorption or emission feature requires only a single term in the sum, which greatly simplifies the analysis. Other macroscopic variables are averaged over the beam line of sight via integration of the path length through the material, i.e., they are geometry dependent integrated quantities.

The macroscopic variables appear as terms and factors in the equation of transfer, a differential equation that describes the change in the specific intensity as a function of position and time in the gas. Applied to a specific line of sight under the condition of pure absorption, the equation of transfer and its solution are greatly simplified. Here, we provide only the most rudimentary essentials required to formulate the radiative transfer solution for a beam of light incident upon an absorbing structure.

4.3.1 Extinction coefficient

As radiation propagates through matter from one physical location to another, the specific intensity can suffer extinction. Along the propagation direction, some of the photons may be deflected by scattering. Alternatively, some of the photons may be *removed* from the radiation field via absorption.

The extinction coefficient, χ_λ, also called the opacity or the total absorption coefficient, is a macroscopic quantity describing the mean reduction of energy removed along a direction of propagation. The extinction coefficient is defined such that the amount of energy $d\epsilon_\lambda$ associated with the specific intensity propagating distance ds in time interval $t \rightarrow t + dt$ is mitigated according to

$$dE_\lambda = \chi_\lambda \, d\epsilon_\lambda \, ds \tag{4.23}$$

where $d\epsilon_\lambda$ is given by Eq. 4.8. We have

$$dE_\lambda = \chi_\lambda \left\{ \mathcal{I}_\lambda \, dA \; d\Omega \, d\lambda \, dt \right\} ds. \tag{4.24}$$

Thus, the extinction coefficient is defined such that a volume element of material of cross section dA and length ds through which radiation of specific intensity

$\mathcal{I}_\lambda$ is propagating will remove energy dE_λ from the radiation field in the solid angle $d\Omega$ in the wavelength range $\lambda \rightarrow \lambda + d\lambda$ in time interval dt. The units of χ_λ are [cm^{-1}].

In order to make a distinction between absorption and scattering, the extinction coefficient is often written as the sum of an absorption coefficient, κ_λ, and a scattering coefficient, σ_λ,

$$\chi_\lambda = \kappa_\lambda + \sigma_\lambda. \tag{4.25}$$

The absorption and scattering coefficients are functions of the absorption and scattering cross sections. A cross section (discussed in § 4.3.2) is defined as the ratio of the power [erg sec^{-1}] removed from the propagation direction by the absorber/scatterer to the incident flux [erg cm^{-2} sec^{-1}]. As such, cross sections can by loosely visualized (for intuitive purposes) as the projected area of interaction for the individual absorber/scatterer.

4.3.2 Cross sections

The working definition of a cross section is derived from a classical picture of particle interactions. Because interactions are probabalistic by nature, and because measurements are by their nature measuring the time averages of countless events, it is useful to describe the behavior using statistical means.

As illustrated in Figure 4.6, consider a beam of cross sectional area A_b comprising monoenergetic particles with particle density n_b moving at velocity v_b. In unit time interval dt, the beam particle flux across a surface perpendicular to the beam is

$$F_b = \frac{1}{A_b}\frac{dN_b}{dt} = \frac{n_b(A_b v_b dt)}{A_b dt} = n_b v_b, \tag{4.26}$$

where $dN_b = n_b(A_b v_b dt)$ is the number of particles in the beam volume element $A_b v_b dt$ crossing the surface. Let the perpendicular surface be a target of thickness L and particle density $n_{\rm T}$. The number of target particles that can potentially interact with any single beam particle is $N_{\rm T} = n_{\rm T} A_b L$. In Figure 4.6*a*, the particles represented by $N_{\rm T}$ are the filled points residing in the target area encompassed by the beam area. From the point of view of the incoming beam, as illustrated in Figure 4.6*b*, if the projected "interaction area" of a target particle is σ, then each potentially interacting target particle has fractional interaction area σ/A_b.

The probability that a single beam particle will interact with a target particle is simply the product of the number of potentially interacting target particles and the fractional interaction area per particle, $N_{\rm T}(\sigma/A_b)$. Geometrically, this is the ratio of the total interaction area of all potentially interacting target particles to the beam cross sectional area (see Figure 4.6*b*). This probability can also be expressed as the ratio of the number of *interacting* beam particles per unit time, $d\mathcal{N}/dt$, to the number of incident beam particles per unit time, dN_b/dt. Equating, we have

$$\frac{d\mathcal{N}/dt}{dN_b/dt} = N_{\rm T}\frac{\sigma}{A_b}. \tag{4.27}$$

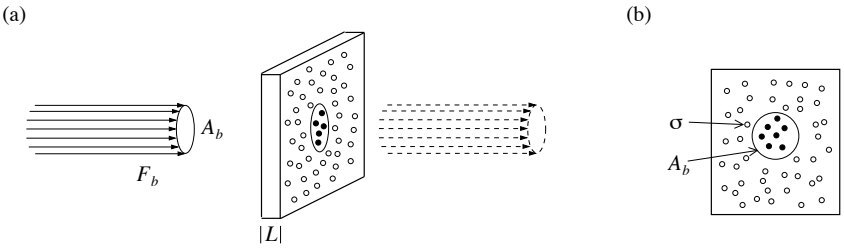

Figure 4.6: (*a*) The schematic of an incident beam of cross sectional area A_b striking a target of thickness L. The beam flux is $F_b = n_b v_b$, where n_b is the particle density and v_b is the velocity of the particles. The number of potentially interacting target particles (shown as filled points) is $N_{\rm T} = n_{\rm T} A_b L$, where $n_{\rm T}$ is the density of target particles. For absorption, the post–target beam flux is reduced, as illustrated with the dashed lines. (*b*) The face–on view of the target illustrating the projected area of the beam (region over which interactions can take place) and the target particle cross section, σ, which is the effective interaction area of a target particle.

We have assumed that a given beam particle can interact with only a single target particle (once a beam particle is absorbed or scattered it is removed from the beam) and that no target particle is shadowed by other target particles. Rearranging, we obtain the statistical definition of the cross section,

$$N_{\rm T}\sigma = \frac{d\mathcal{N}/dt}{(1/A_b)(dN_b/dt)} = \frac{\mathcal{P}}{F_b}, \tag{4.28}$$

where $\mathcal{P} = d\mathcal{N}/dt$ has been invoked for the beam particle interaction rate (power removed from the beam) and $F_b = (1/A_b)(dN_b/dt)$ has been invoked for the beam particle flux (Eq. 4.26). Since the units of $\mathcal{P}$ are [particles sec^{-1}] and the units of F_b are [particles cm^{-2} sec^{-1}], we find that the units of $N_{\rm T}\sigma$ are [cm^2]. Thus, the units of the cross section are *per potential target particle*, [cm^2 particle^{-1}].

In words, σ is the ratio of the number of interacting beam particles per unit time per potential target particle to the particle flux of the beam. Stated slighty differently, σ is the ratio of the power at which particles are removed from the beam per potential target particle to the particle flux of the beam, or

$$\sigma = \frac{\text{power removed from beam per target particle}}{\text{flux of incident beam}}. \tag{4.29}$$

Pure absorption

If the interation process is purely absorption, then the post–target beam has a reduced particle density. This is schematically illustrated in Figure 4.6*a* where the dashed lines representing the beam after passing through the target indicate the reduced flux. We assume there is no scattering, only the absorption and removal of particles from the beam. If the number of particles in a unit volume of the beam following interaction with the target is $N_b - dN_b$, then the rate

at which particles are removed from the beam is $\mathcal{P} = -dN_b/dt = -A_b dF_b$, where the last step follows from Eq. 4.26. Substituting into Eq. 4.28 yields $N_{\rm T}\sigma = -A_b(dF_b/F_b)$. From $N_{\rm T} = n_{\rm T}A_b L$, and rearranging, we obtain

$$\frac{dF_b}{F_b} = -n_{\rm T}\sigma L, \tag{4.30}$$

a differential equation with solution

$$F_b = F_b^0 \exp\left\{-n_{\rm T}\sigma L\right\}, \tag{4.31}$$

where F_b is the post–target beam flux and F_b^0 is the beam flux incident on the target (the boundary condition). Note that the product $n_{\rm T}L = N_{\rm T}/A_b = N$ is the column density (see Eq. 5.13) of potentially interacting target particles. Eq. 4.31 is directly analogous to the formalism employed in § 5.2 to describe the reduction of intensity from a beam of light in terms of the column density of absorbers, N, and the atomic cross section, $\alpha(\lambda)$, as expressed in Eq. 5.15.

In fact, if the particles in the beam are photons of wavelength λ, then the particle flux, $F_b = n_b v_b$, can be replaced by the radiative energy flux. This is most simply accomplished by substituting the radiative energy density, $n_\epsilon(\lambda)$, for the particle density, n_b, and substituting $v_b = c$ for the velocity in Eq. 4.26,

$$F_b(\lambda) = n_\epsilon(\lambda)\, c = \mathcal{I}_\lambda^0. \tag{4.32}$$

Following the identical treatment used to obtain Eq. 4.31 for a particle beam, we find that the absorption of specific intensity in a radiative beam obeys,

$$\mathcal{I}_\lambda = \mathcal{I}_\lambda^0 \exp\left\{-N\sigma(\lambda)\right\}, \tag{4.33}$$

where $N = n_{\rm T}L$ is the column density and the absorption cross section at wavelengh λ is $\sigma(\lambda)$.

As defined in Eq. 4.33, the cross section applies for the finite wavelength range $\lambda \rightarrow \lambda + d\lambda$. This requires a slight modification to the definition of Eq. 4.29. For a photon beam, it is the integral of $\sigma(\lambda)$ over wavelength that provides the fractional power removed from the beam,

$$\sigma = \int_0^\infty \sigma(\lambda)\, d\lambda = \frac{\text{power removed from beam per target particle}}{\text{flux of incident beam}}. \tag{4.34}$$

4.3.3 Incorporating atomic absorption cross section

Consider the absorption coefficient component to the extinction coefficient, κ_λ. The magnitude of the absorption at any location in a gas depends upon the number density of *potential* "absorbers" and may vary significantly with wavelength. Here, we emphasize that an absorber is an atom of species k that is in one of all possible ionization stages, j, and excitation states, i.

The chance that a photon of wavelength λ will be absorbed by any single potential absorber in state ijk is described by a wavelength dependent absorption cross section, $\alpha_{ijk}(\lambda)$, which has units [cm^2 absorbers^{-1}]. If the number

density of the potential absorber in state ijk is n_{ijk} [absorbers cm^{-3}], then this absorber contributes $n_{ijk}\alpha_{ijk}(\lambda)$ to the total absorption coefficent at wavelength λ. The total absorption coefficient is the sum over all possible absorbers of the product of the absorption cross section per absorber and the number density of absorbers,

$$\kappa_\lambda = \sum_{ijk} n_{ijk}\, \alpha_{ijk}(\lambda). \tag{4.35}$$

The two main types of atomic absorption are (1) bound–bound, where a photon is absorbed by an electron that is elevated in energy from one orbit to another within an atom, and (2) bound–free, where a photon is absorbed in the processes of liberating a bound electron from an atom (ionization). The absorption cross sections are derived based upon the principles of atomic physics; each and every cross section is defined for an interaction of photons with a given atomic species in a given ionization stage and excitation state. The $\alpha_{ijk}(\lambda)$ for a given interaction vary only with photon wavelength.

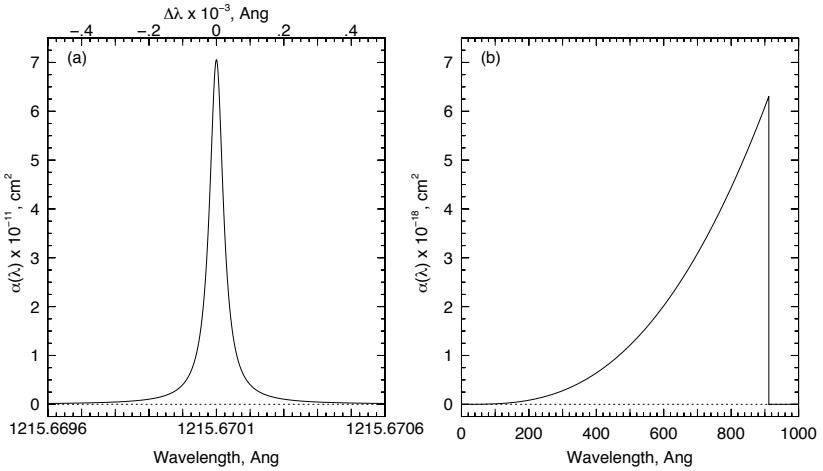

Figure 4.7: Two selected absorption cross sections for neutral hydrogen in the ground state. (*a*) The bound–bound absorption cross section for the Lyα λ1215 transition, which peaks at 1215.6701 Å. (*b*) The bound–free absorption cross section for ionization from the ground state, which is possible only for photons having wavelengths less than $\simeq$ 912 Å.

Examples of a bound–bound and a bound–free absorption cross section are presented in Figures 4.7*a* and 4.7*b*, respectively, for ground–state neutral hydrogen. As illustrated, in the case of any single particular atomic bound–bound transition, $\alpha(\lambda)$ is highly peaked over a very narrow wavelength range, on the order of $\Delta\lambda \simeq 10^{-4}$ Å. In the case of ionization, all photons having energy less than the energy required to liberate the bound electron have $\alpha(\lambda) = 0$, whereas all photons having energy equal to or greater than the energy required to liberate the bound electron have a finite cross section for ionization. For these "ionizing photons", $\alpha(\lambda)$ varies smoothly with wavelength. However, there is an abrupt transition in the magnitude of $\alpha(\lambda)$ at the wavelength where ionization can be

first be achieved. This is known as an "ionization edge".

4.3.4 Optical depth

The inverse of the extinction coefficient is the mean free path,

$$\ell_\lambda = \chi_\lambda^{-1}, \tag{4.36}$$

which is the average distance a photon of wavelength λ propagates before it is absorbed or scattered from the $\hat{\mathbf{s}}$ direction. We now define the absorptivity along the path length element ds as $d\tau_\lambda = \chi_\lambda\, ds$. The optical depth is defined as the integrated absorptivity along the path length. In general, the optical depth from location s_1 to location s_2 is

$$\tau_\lambda = \int_{s_1}^{s_2} \chi_\lambda\, ds, \tag{4.37}$$

where s_1 precedes s_2 along the propagation direction. To obtain the total optical depth along the line of sight through material of finite extent, L, the limits of integration become $s_1 = 0$ and $s_2 = L$. The difficulty in determining the optical depth using Eq. 4.37 is that χ_λ may vary with physical location in the material (and therefore path length location) in an unknown way.

The integrand of Eq. 4.37 is equivalent to the ratio of the path length element to the mean free path, ds/ℓ_λ. Thus, the optical depth is interpreted as the most probable number of mean free paths that a photon of wavelength λ will travel before being absorber or scattered out of its direction of propagation.

Optical "thickness"

Commonly, the term "optically thin" is employed to describe material with $\tau_\lambda < 1$ and "optically thick" is employed for $\tau_\lambda \geq 1$. For an optically thin medium, the total path length through the material is less than the free mean path of the photons. For an optically thick medium, the total path length through the medium is equal to or greater than the mean free path of the photons.

Two caveats are in order: (1) since optical depth varies with wavelength, the material may be optically thick to certain photons, but optically thin to others (even in a narrow wavelength range, such as across a single absorption profile or feature), and (2) the material may be optically thick to certain types of aborption/scattering processes, but optically thin to others. Thus, the terms "optically thin" and "optically thick" are applied in the context of the wavelengths of the photons be addressed.

4.3.5 Emission coefficient and source function

The incremental emission of radiative energy dE_λ from a volume element of material of cross section dA and length ds into the solid angle $d\Omega$ in the wavelength range $\lambda \rightarrow \lambda + d\lambda$ in time interval dt is parameterized by the emission

coefficient, η_λ,

$$dE_\lambda = \eta_\lambda \, dA \, ds \, d\Omega \, d\lambda \, dt, \tag{4.38}$$

where η_λ has units [erg cm^{-3} rad^{-2} Å^{-1} sec^{-1}].

In a steady state thermal equilibrium for which there is no net energy gain or loss in the material, the energy increment due to emission equals the energy decrement due to absorption (excluding scattering),

$$\eta_\lambda \, dA \, ds \, d\Omega \, d\lambda = \kappa_\lambda \left\{ \mathcal{I}_\lambda \, dA \; d\Omega \, d\lambda \right\} ds, \tag{4.39}$$

which simplifies to

$$\eta_\lambda = \kappa_\lambda \mathcal{I}_\lambda. \tag{4.40}$$

This relation states that in thermal equilibrium, and in the absence of an external radiation source, the ratio of the emission coefficient to the absorption component of the extinction coefficient is the net specific intensity in the material.

In general, the ratio of the emission coefficient to the extinction coefficient,

$$S_\lambda = \frac{\eta_\lambda}{\chi_\lambda} = \frac{\eta_\lambda}{\kappa_\lambda + \sigma_\lambda}, \tag{4.41}$$

is called the source function, which has the units of specific intensity [erg cm^{-2} rad^{-2} Å^{-1} sec^{-1}]. The source function is a convenient quantity for describing the net specific intensity emitted into the medium under general thermodynamic conditions.

4.4 Transfer equation

The generalized equation of radiative transfer is

$$\frac{1}{c} \frac{\partial \mathcal{I}_\lambda}{\partial t} + \hat{\mathbf{s}} \cdot \nabla \mathcal{I}_\lambda = \eta_\lambda - \chi_\lambda \mathcal{I}_\lambda. \tag{4.42}$$

The first term on the left accounts for the spatial change in the specific intensity due to the rate of temporal changes in the radiation field. The second term on the left accounts for the observed (line of sight) component of the gradient of the specific intensity. These rates of change are equal the difference between the local source of the specific intensity, η_λ, less the specific intensity remaining following extinction, $\chi_\lambda \mathcal{I}_\lambda$.

Dividing by the extinction coefficient (equivalent to multiplying by the mean free path), we obtain

$$\frac{1}{\chi_\lambda} \left[\frac{1}{c} \frac{\partial \mathcal{I}_\lambda}{\partial t} + \hat{\mathbf{s}} \cdot \nabla \mathcal{I}_\lambda \right] = S_\lambda - \mathcal{I}_\lambda, \tag{4.43}$$

where S_λ is the source function (Eq. 4.41). Expressed in Cartesian coordinates, we have

$$\hat{\mathbf{s}} \cdot \nabla \mathcal{I}_\lambda = (\hat{\mathbf{s}} \cdot \hat{\mathbf{i}}) \, \frac{\partial \mathcal{I}_\lambda}{\partial x} + (\hat{\mathbf{s}} \cdot \hat{\mathbf{j}}) \, \frac{\partial \mathcal{I}_\lambda}{\partial y} + (\hat{\mathbf{s}} \cdot \hat{\mathbf{k}}) \, \frac{\partial \mathcal{I}_\lambda}{\partial z}, \tag{4.44}$$

and expressed in spherical coordinates, we have

$$\hat{\mathbf{s}} \cdot \nabla \mathcal{I}_\lambda = (\hat{\mathbf{s}} \cdot \hat{\mathbf{r}}) \frac{\partial \mathcal{I}_\lambda}{\partial r} + (\hat{\mathbf{s}} \cdot \hat{\mathbf{\Theta}}) \frac{\partial \mathcal{I}_\lambda}{r\, \partial \theta} + (\hat{\mathbf{s}} \cdot \hat{\mathbf{\Phi}}) \frac{\partial \mathcal{I}_\lambda}{r \sin\theta\, \partial \phi}. \tag{4.45}$$

4.4.1 Pure absorption in 1–D

In the scenario of quasar absorption line studies of intervening absorbers, the only known geometric information is the line of sight direction to the quasar. It is common practice to assume a plane parallel geometry.

Consider a one dimensional gas "cloud" of thickness L'. Let the depth into the cloud be measured by the coordinate z in the Cartesian system, where $z = 0$ is the cloud "face". Further, assume the photon propagation direction (line of sight being measured) is $\hat{\mathbf{s}}$, such that $\hat{\mathbf{s}} \cdot \hat{\mathbf{k}} = \cos\theta$. A schematic of the scenario is illustrated in Figure 4.8. The boundary condition is that specific intensity $\mathcal{I}_\lambda(0)$ is incident on the cloud face. For steady state conditions, the equation of transfer for this scenario is written

$$\frac{(\hat{\mathbf{s}} \cdot \hat{\mathbf{k}})}{\chi_\lambda(z)} \frac{d\mathcal{I}_\lambda(z)}{dz} = \cos\theta \frac{d\mathcal{I}_\lambda(z)}{\chi_\lambda(z)\, dz} = S_\lambda(z) - \mathcal{I}_\lambda(z). \tag{4.46}$$

Invoking the definition of the absorptivity, we have $d\tau_\lambda = \chi_\lambda(z)\, ds$, and accounting for the propagation direction with respect to the geometric coordinate, we obtain $d\tau_\lambda = \chi_\lambda(z)\, dz / \cos\theta$. From Eq. 4.37, we have

$$\tau_\lambda(z) = \frac{1}{\cos\theta} \int_0^z \chi_\lambda(z)\, dz. \tag{4.47}$$

Since τ_λ and z have a monotonic functional relationship, we can rewrite the transfer equation as a function of the optical depth as the independent variable,

$$\frac{d\mathcal{I}_\lambda(\tau_\lambda)}{d\tau_\lambda} = S_\lambda(\tau_\lambda) - \mathcal{I}_\lambda(\tau_\lambda). \tag{4.48}$$

Employing the optical depth as the independent variable in Eq. 4.48 may seem somewhat less intuitive than solving the transfer equation as a function of physical depth. However, in practice, the transfer equation is simply a tool applied to observational spectra, which directly provide the optical depth as a function of wavelength.

For absorption line studies, it is almost always true (or assumed) that there is no emission within the cloud, i.e., $S_\lambda(\tau_\lambda) = 0$ (a pure absorbing cloud). For this condition, and applying the boundary condition on the cloud face, the solution to Eq. 4.48 is

$$\mathcal{I}_\lambda(\tau_\lambda) = \mathcal{I}_\lambda(0) \exp\{-\tau_\lambda\}. \tag{4.49}$$

Eq. 4.49 is the workhorse expression for analysis of absorption line features in astronomical spectra.

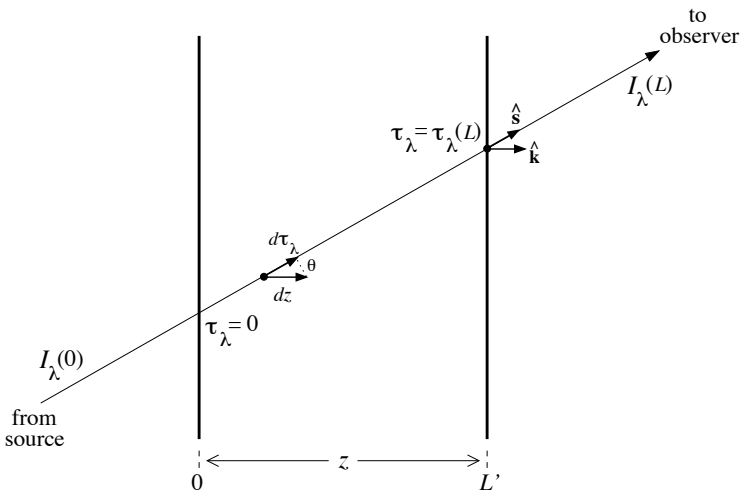

Figure 4.8: Schematic of a one dimensional plane parallel "cloud" of physical thickness L' through which a beam of specific intensity $\mathcal{I}_\lambda(z)$ is propagating in the $\hat{\mathbf{s}}$ direction such that $\hat{\mathbf{s}} \cdot \hat{\mathbf{k}} = \cos\theta$, where $\hat{\mathbf{k}}$ is the unit vector along the geometric axis of the cloud. The specific intensity at an optical depth τ_λ measured from the cloud "face" ($\tau_\lambda = 0$) is the extinction $\mathcal{I}_\lambda(0)\exp\{-\tau_\lambda\}$ of the incident specific intensity under the assumption that $S_\lambda(\tau_\lambda) = 0$.

4.4.2 Interpretation

For illustration, assume a path length averaged extinction coefficient, $\bar{\chi}_\lambda$. Evaluating Eq. 4.47 with $s_1 = 0$ and $s_2 = s$, we have $\tau_\lambda = \bar{\chi}_\lambda\, s$, were $s = z/\cos\theta$ is the coordinate position along the line of sight. Eq. 4.49 can now be written as a function of the path length s,

$$\mathcal{I}_\lambda(s) = \mathcal{I}_\lambda(0)\exp\{-\bar{\chi}_\lambda\, s\}\,. \tag{4.50}$$

When $s = \bar{\chi}_\lambda^{-1}$, the photons have traveled one complete mean free path and the specific intensity has suffered extinction by the factor $e^{-1} = 0.367$. For every multiple additional mean free path the beam travels, the extinction is an additional factor of 0.367. If a beam travels the full distance $s = L = L'/\cos\theta$ through the absorbing cloud, then the total optical depth of the cloud is $\tau_\lambda = \bar{\chi}_\lambda\, L$.

In Figure 4.9*a*, the behavior of Eq. 4.50 is illustrated as a function of path length for four different $\bar{\chi}_\lambda$ in an absorbing cloud through which the total path length is L. The different extinction coefficients result in different extinction rates and therefore in different total optical depths, τ_λ. The four cases are for $\tau_\lambda = 0.5$, 1.0, 2.0, and 4.0. The ratios of the specific intensity of the emerging beam to the incident beam, $\mathcal{I}_\lambda(s \geq L)/\mathcal{I}_\lambda(0)$, are given for the four total optical depths.

In Figure 4.9*b*, an idealized absorption profile is shown. In this example, the absorption profile is the manifestation of the wavelength dependence of $\bar{\chi}_\lambda$, which results in a total optical depth that varies with wavelength in a single

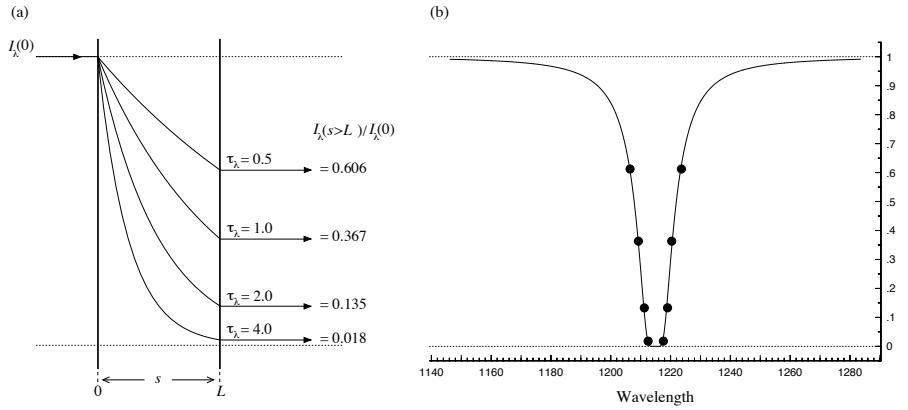

Figure 4.9: (*a*) A schematic of radiative transfer through a pure absorbing cloud, i.e., $S_\lambda(\tau_\lambda) = 0$, of total path length L, for which the total optical depth is $\tau_\lambda = 0.5$, 1.0, 2.0, and 4.0, depending upon wavelength. The incoming beam $\mathcal{I}_\lambda(0)$ (propagating from left to right) suffers extinction through the cloud according to Eq. 4.50. Since τ_λ is the integral of $\bar{\chi}_\lambda$ over the path length from $0 \leq s \leq L$, the examples are for different opacities at different wavelengths. (*b*) An example absorption profile, $\mathcal{I}_\lambda(s>L))/\mathcal{I}_\lambda(0)$. The filled points superimposed on the profile correspond to the four example τ_λ values.

cloud structure. The intensity and wavelength values along the profile that correspond to the four example total optical depths are represented by filled points superimposed on the profile. Photons with wavelengths near the profile center are more readily absorbed. Where $\tau_\lambda \geq 1$, the path length through the cloud for these photons is equal to or greater than the photon mean free paths, i.e., the cloud is optically thick. Near the profile wings, $\tau_\lambda < 1$ and the photon path lengths through the cloud are less than a single mean free path, i.e., the cloud is optically thin.

References

Emerson, D. 1996, *Interpreting Astronomical Spectra*, John Wiley & Sons

Gray, D. F. 1992, *The Observational and Analysis of Stellar Photospheres*, Cambridge University Press

Mihalas, D. 1978, *Stellar Atmospheres*, W. H. Freeman & Company

Novotny, E. 1973, *Introduction to Stellar Atmospheres and Interiors*, W. H. Freeman & Company

Peraiah, A. 2002, *An Introduction to Radiative Transfer: Methods and Applications in Astrophysics*, Cambridge University Press

Rybicki, G. B, & Lightman, A. P. 2004, *Radiative Processes in Astrophysics*, Wiley–VCH Verlag GmbH & Company

Shu, F. H. 1991, *The Physics of Astrophysics I.: Radiation*, University Science Books